The paper was published in the proceedings of the 6th International Conference on Geotechnical and Geophysical Site Characterization and was edited by Tamás Huszák, András Mahler and Edina Koch. The conference was originally scheduled to be held in Budapest, Hungary in 2020, but due to the COVID-19 pandemic, it was held online from September 26th to September 29th 2021.

Liquefaction assessment through SCPTu and DMT tests: Aveiro case study

Diana Cordeiro
CONSTRUCT-GEO, Engineering Faculty, University of Porto, Porto, Portugal, ec12020@fe.up.pt

António Viana da Fonseca[1], Cristiana Ferreira[2], Fausto Molina-Gómez[3]
CONSTRUCT-GEO, Engineering Faculty, University of Porto, Porto, Portugal, viana@fe.up.pt[1], cristiana@fe.up.pt[2], fausto@fe.up.pt[3]

Carlos Rodrigues
Polytechnic Institute of Guarda, Guarda, Portugal, crod@ipg.pt

ABSTRACT: Cone Penetration Tests (CPT) and Flat Marchetti Dilatometer (DMT) are two of the most valuable in situ tests used in soil investigations. An experimental campaign for site characterization was performed in Aveiro (Portugal), including seismic piezocone (SCPTu) and flat dilatometer (DMT) tests, for the purpose of liquefaction susceptibility assessment. In this campaign, sandy soils with fine silt-clayey interlayers were identified. This paper presents the CPTu and DMT results, their inferred soil parameters and their influence in the estimate of the cyclic resistance ratio (CRR), derived from the normalized cone resistance ($Q_{tn,cs}$) and the horizontal stress index (K_D). The factor of safety against liquefaction (FS_{liq}) was obtained from cyclic stress ratio (CSR) determined for the specific seismic actions according to Eurocode 8, allowing to derive liquefaction damage indices, LPI and LSN.

Keywords: penetration testing (SCPTu and DMT), geotechnical parameters, liquefaction

1. Introduction

Soil liquefaction is a phenomenon that can result from seismic activity and leads to a drastic decrease of the strength and stiffness of the soil, and even its annulment, as an outcome of the pore pressure build-up.

Liquefaction is mainly associated with loose granular soils below ground water table and it can result in catastrophic consequences such as dam collapse, slope instability, high settlements of structures, collapse of retaining wall structures, among others. The assessment of the liquefaction potential can be based on several distinct in situ tests and laboratory experiments.

Within the scope of the research project PTDC/ECM-Geo/1780/2014 entitled "Liquefaction Assessment Protocols to Protect Critical Infrastructures Against Earthquake Damage (LIQ2PROEARTH)", a set of in situ tests were performed in Aveiro (Portugal) in order to gather field geotechnical information to be used in the evaluation of the liquefaction conditions.

2. Site Investigations

This paper focuses on the assessment of liquefaction susceptibility at the Barra Bridge surrounding grounds, located in Aveiro, on the North-Western coast of Portugal. Even though the seismic hazard of the region is low, the presence of a sensitive structure, such as the bridge in question, required specific ground characterization.

The Aveiro region is part of an extensive coastal plain with a NW-SE orientation, low altitude and high topographic uniformity. On shore, geology reveals recent dune, beach and lagoon sediments, characterized as alluvial Holocene deposits, which lay on Cretaceous and Plio-Pleistocene materials. The Aveiro test site is mainly composed by sand with thin interlayers of silt and clay with organic matter.

For this site investigation campaign, three cone penetration tests (CPTu) and three dilatometer tests (DMT) were conducted. Fig. 1. shows the experimental site, which is located next to the mentioned area. During the execution of the tests, the ground water levels fluctuated between the depths of 0.3 m and 1.8 m as a result of the tides. Fig. 2. shows the profiles with depth of the CPTu measured parameters such as: the cone resistance q_c, the sleeve friction f_s, the pore pressure u_2 and soil behavior type index Ic; and the material index I_D as a DMT parameter for the different sites.

Figure 1. Map of the experimental site and location of the SCPTu and DMT tests

3. Liquefaction Assessment

The "Simplified Procedure", originally introduced by Seed & Idriss [1], is the most common method in the assessment of liquefaction susceptibility. This procedure is based on the estimate of the safety factor against lique-

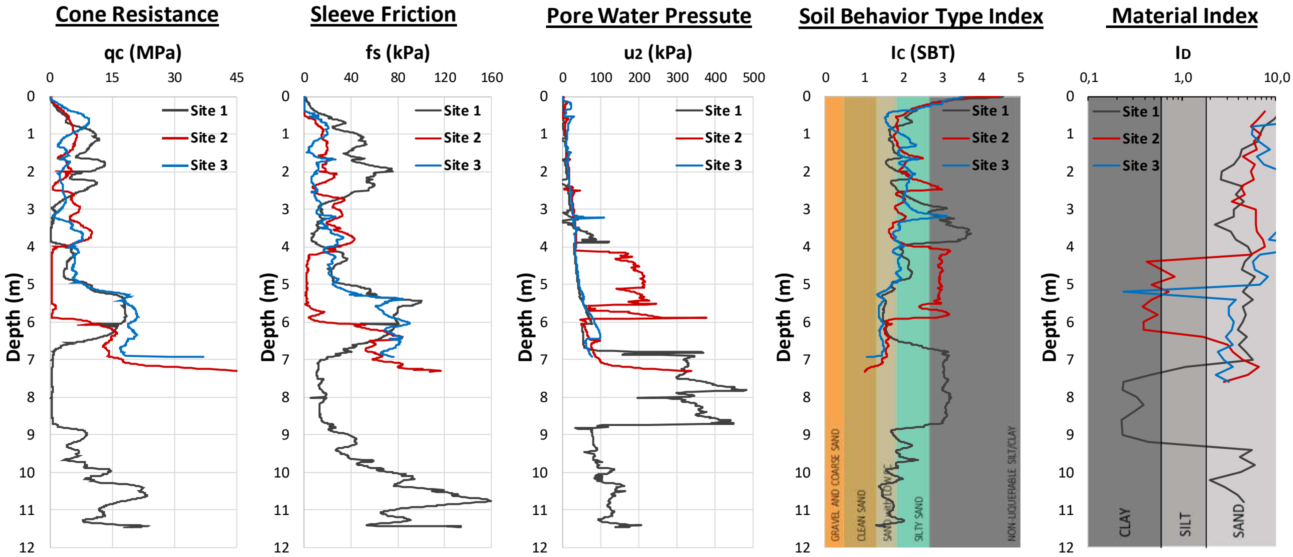

Figure 2. CPTu and DMT results for the three different sites

faction (FS_{liq}), which relates the cyclic resistance ratio (CRR) with the cyclic stress ratio (CSR), as follows:

$$FS_{liq} = \frac{CRR}{CSR} \quad (1)$$

The cyclic stress ratio evaluates the expected seismic action loading on the soil layers and can be determined from the design peak ground acceleration at the specific location, according to Eurocode 8. On the other hand, the cyclic resistance ratio refers to the capacity of the soil, at a given depth, to resist liquefaction, and it can be inferred from different in situ techniques and parameters.

As alternative approaches to liquefaction assessment, quantitative liquefaction risk indexes can be estimated, such as the liquefaction potential index (LPI) and the liquefaction severity number (LSN), in order to quantify the effects of liquefaction and consequent land damage.

Iwasaki et al. [2] introduced the LPI to estimate the site vulnerability to liquefaction effects, by combining the safety factor with a linear function of depth, as shown in Eq. 2 to 4. The classification of liquefaction potential based on the LPI index can be made according to Table 1.

$$LPI = \int_0^{20} F \cdot w(z)\, dz \quad (2)$$

where F is a function of the safety factor obtained from the simplified liquefaction evaluation procedure defined in Eq. (1):

$$F = \begin{cases} 1 - FS_{liq}, & FS_{liq} \leq 1 \\ 0, & FS_{liq} > 1 \end{cases} \quad (3)$$

and $w(z)$ a function of the depth below ground surface, z:

$$w(z) = 10 - 0.5z \quad (4)$$

Table 1. Classification of liquefaction potential based on LPI [3]

Liquefaction potential	LPI
Very Low	0
Low	0 < LPI ≤ 5
High	5 < LPI ≤ 15
Very High	>15

The liquefaction severity number, LSN, developed by Tonkin & Taylor [4], is an indicator of the possible liquefaction consequences. It represents the expected damage effects of ground liquefaction on shallow foundations based on post-liquefaction reconsolidation settlements, and is formulated as follows:

$$LSN = 1000 \int \frac{\varepsilon_V}{z}\, dz \quad (5)$$

where z is the depth of a certain layer below ground surface and ε_V is the post-liquefaction volumetric strain densification of that layer calculated according to Zhang [5]. The expected damage effects can be categorized by the different ranges of LSN, presented in Table 2.

Table 2. LSN ranges for the liquefaction land effects [4]

LSN	Damage effects
0 < LSN ≤ 10	Little to no expression of liquefaction
10 < LSN ≤ 20	Minor expression of liquefaction, some sand boils
20 < LSN ≤ 30	Moderate expression of liquefaction, with sand boils and some structural damage
30 < LSN ≤ 40	Moderate to severe expression of liquefaction, settlement can cause structural damage
40 < LSN ≤ 50	Major expression of liquefaction, undulations and damage to ground surface, severe total and differential settlement of structures
LSN > 50	Severe damage, extensive evidence of liquefaction at surface, severe total and differential settlement affecting structures, damage to services

3.1. Cyclic Stress Ratio (CSR)

The calculation of the cyclic stress ratio generated by an earthquake was estimated using Seed and Idriss [1] proposal (see Eq. 6), considering the shear stress reduction coefficient (r_d), the magnitude scaling factor (MSF) and the overburden correction factor (K_σ).

$$CSR = 0.65 \cdot \frac{a_{max}}{g} \cdot \frac{\sigma_{vo}}{\sigma'_{vo}} \cdot r_d \cdot \frac{1}{MSF} \cdot \frac{1}{K_\sigma} \quad (6)$$

where a_{max} is the peak horizontal acceleration at the ground site, g the gravity acceleration, σ_{v0} and σ'_{v0} are the total and effective vertical stress at a specific depth.

The peak horizontal acceleration, a_{max}, was defined considering the two seismic scenarios introduced in the Portuguese National Annex of the Eurocode 8 [6,7]:

- *Seismic Action 1*: characterized by earthquakes mainly with offshore epicenters (far source), low predominant earthquake frequency, high magnitude and long duration.
- *Seismic Action 2*: characterized by earthquakes mainly with inland epicenters (near source), high predominant earthquake frequency, moderate magnitude and short duration.

The main parameters that characterize the two seismic actions for the Aveiro site are summarized in Table 3, such as the seismic zones, the return period T_R, the moment magnitude M_w, and the peak horizontal acceleration at the ground surface a_{max}.

Table 3. Aveiro site seismic actions

	Seismic Action 1	**Seismic Action 2**
Seismic Zone	1.6	2.4
T_R (years)	475	475
M_w	7.2	4.4
a_{max} (m/s^2)	0.7	2.2

The shear stress reduction coefficient r_d, that accounts for the dynamic response of the soil profile, was calculated according to Idriss [8] formulation:

$$r_d = e^{[\alpha(z)+\beta(z)\cdot M]} \quad (7)$$

with $\alpha = -1.012 - 1.126 \cdot sin\left(\frac{z}{11.73} + 5.133\right)$ (8)

and $\beta = 0.106 + 0.118 \cdot sin\left(\frac{z}{11.28} + 5.142\right)$ (9)

where z is the depth and M the earthquake magnitude.

The magnitude scaling factor (*MSF*) is used to account for the duration effects on the triggering of liquefaction, namely the number and relative amplitudes of loading cycles. According to [8], *MSF* can be calculated as follows:

$$MSF = 6.9 \cdot exp\left(-\frac{M}{4}\right) - 0.058 \leq 1.8 \quad (10)$$

The overburden correction factor K_σ is a function of the effective consolidation stress, and can be determined through Idriss & Boulanger [9] relationship:

$$K_\sigma = 1 - C_\sigma \cdot ln\left(\frac{\sigma'_{v0}}{P_a}\right) \leq 1.1 \quad (11)$$

with $C_\sigma = \frac{1}{37.3-8{,}27\cdot(q_{c1Ncs})} \leq 0.3$ (12)

where P_a is the atmospheric pressure and D_r the relative density.

3.2. Cyclic Resistance Ratio (CRR)

The cyclic resistance ratio can be evaluated from different in situ tests and laboratory results for a more reliable outcome. For the Aveiro test site, the capacity of the soil to resist liquefaction was derived from CPTu and DMT measurements, which are particularly convenient due to the extensive worldwide database and past experience.

3.2.1. CPTu Tests

The CRR estimated from the CPTu data followed the correlation established by Boulanger & Idriss [10] that considers, at each depth, the normalized equivalent clean sand cone resistance q_{c1Ncs}, as below:

$$CRR = \exp\left[\frac{q_{c1Ncs}}{113} + \left(\frac{q_{c1Ncs}}{1000}\right)^2 - \left(\frac{q_{c1Ncs}}{140}\right)^3 + \left(\frac{q_{c1Ncs}}{137}\right)^4 - 2.80\right] \quad (13)$$

with $q_{c1Ncs} = K_C \cdot Q_{tn}$ (14)

where K_c is a correction factor that is a function of grain characteristics of the soil that can be estimated using I_c. $Q_{tn} = [(q_t - \sigma_{vo})/p_a] \cdot (p_a/\sigma'_{v0})^n$ is the normalized cone tip resistance. Fig. 3. presents the normalized equivalent clean sand cone resistance (q_{c1Ncs}) profiles.

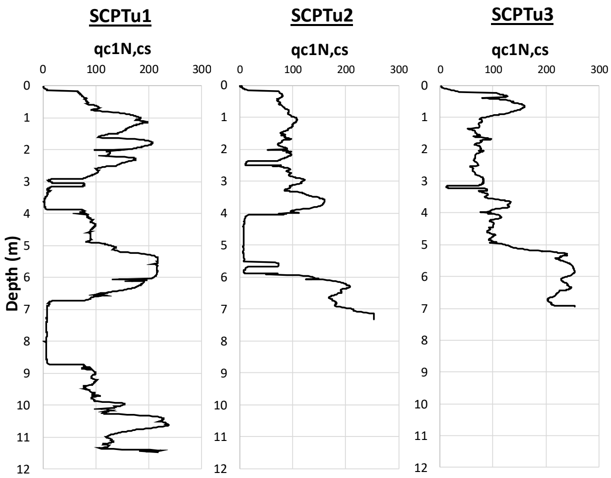

Figure 3. Evolution of the normalized equivalent clean sand cone resistance of the CPTu tests

3.2.2. DMT Tests

The evaluation of the capacity of the soil to resist liquefaction through the dilatometer test is based on the horizontal stress index $K_D = (P_0 - u_0)/\sigma'_{v0}$. It has been observed that K_D is more sensitive to factors that increase the liquefaction resistance besides relative density D_r (which is reflected essentially in the normalized cone tip resistance Q_{cn} given by the CPT tests), such as in situ K_0, stress history, preloading, aging and cementation [11]. Fig. 4. presents the K_D profiles of the studied site.

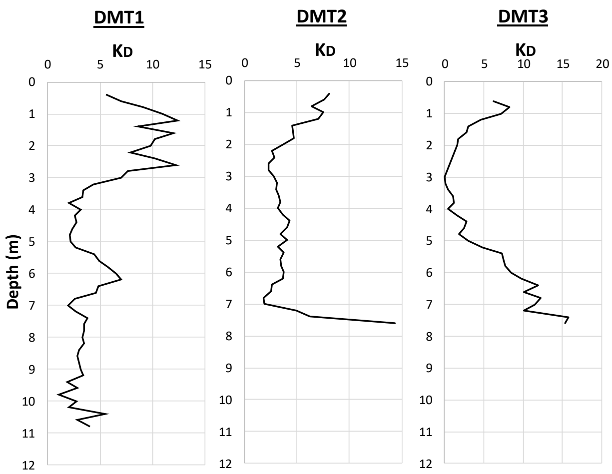

Figure 4. Evolution of the horizontal stress index of the DMT tests

The adopted correlation between CRR- K_D results of the combination of Eq. (15) and (16), which are, respectively, Idriss & Boulanger [12] correlation to estimate CRR using CPT data, and the CPT-DMT relationship given by [13].

$$CRR = \exp\left(\frac{Q_{cn}}{540} + \left(\frac{Q_{cn}}{67}\right)^2 - \left(\frac{Q_{cn}}{80}\right)^3 + \left(\frac{Q_{cn}}{114}\right)^4 - 3\right) \quad (15)$$

$$\text{with } Q_{cn} = 25 \cdot K_D \quad (16)$$

3.3. Liquefaction Assessment Results

The assessment of liquefaction susceptibility was made according to the methodologies presented above. The analyses were carried out according to the "simplified procedure", and the factors of safety against liquefaction were computed for the three locations, based on the CPTu and DMT data. Figs. 5. and 6. features the evolution of FS_{liq} in depth estimated from the piezocone and dilatometer tests considering the seismic action 1 and 2, respectively.

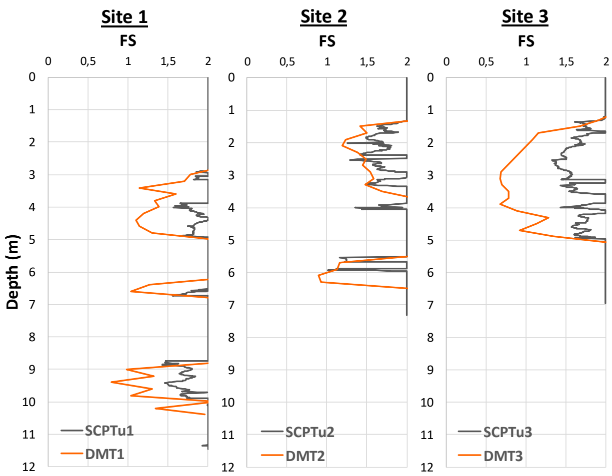

Figure 5. Estimation of the safety factor against liquefaction for SCPTu and DMT test, considering Seismic Action 1

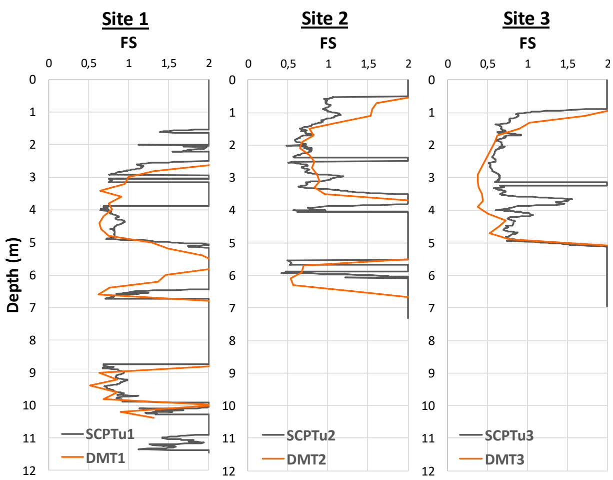

Figure 6. Estimation of the safety factor against liquefaction for SCPTu and DMT test, considering Seismic Action 2

The comparison of the results obtained at the three different sites indicate a good agreement between the two methods, as both identified the same critical layers susceptible to liquefaction, and there is no significant difference between the absolute values of FS_{liq}. It is also noticeable that the seismic action 2 is considerably detrimental than the seismic action 1, due to the higher a_{max}, as the number and thickness of layers that are liquefiable increase significantly.

Quantitative liquefaction risk indicators were also calculated. Tables 4 and 5 present the values of the liquefaction potential index (LPI) and the liquefaction severity number (LSN), considering each seismic action for CPTu and DMT tests, respectively. Comparing the values of LPI and LSN obtained, some differences can be observed, especialy for LSN in the seismic action 2.

Table 4. LPI and LSN values for CPTu tests

	Seismic Action 1		Seismic Action 2	
	LPI	**LSN**	**LPI**	**LSN**
SCPTu1	0.00	0.00	2.98	11.16
SCPTu2	0.00	0.23	5.69	33.02
SCPTu3	0.00	0.03	8.81	41.80

Table 5. LPI and LSN values for DMT tests

	Seismic Action 1		Seismic Action 2	
	LPI	**LSN**	**LPI**	**LSN**
DMT1	0.23	0.23	5.87	1.07
DMT1	0.24	0.19	5.69	1.34
DMT1	5.17	5.71	14.52	6.57

When subjected to Type 1 seismic action, the three soil profiles exhibit very low to low liquefaction potential (LPI≤5) and little to no expression of liquefaction (LSN<10). For seismic action 2, LPI values indicate a high liquefaction potential but there is no agreement between the LSN values obtained from CPTu and DMT tests. While for the piezocone test, the LSN predict minor to major expression of liquefaction, damage ground surface, severe total and differential settlements; for the dilatometer test, it estimates little to no expression of liquefaction.

This discrepancy can be upheld by factors that are not considered in the DMT tests, such as relative density or fines content. For this reason, the fine content of the soil should be measured in the laboratory [14]. It also should be reminded that LPI and LSN are not intended to be reliable indicators of vulnerability in case of significant lateral spreading. Alternate measures that include consideration of lateral spreading are required to make an appropriate assessment of liquefaction land damage [15].

At this purpose, a new approach for the Fragility Assessment of Traffic Embankments due to Earthquake-Induced Liquefaction was proposed in a recently concluded H2020 EU project ("Assessment and mitigation of liquefaction potential across Europe: a holistic approach to protect structures / infrastructures for improved resilience to earthquake-induced liquefaction disasters", www.liquefact.eu). In this work, a large set of fragility curves was derived based on the results of numerical calculations using software package FLAC 2D and PM4Sand material model for simulating the behaviour of the liquefiable layer during dynamic excitation. The width and height of the embankment, thickness and density state of the liquefiable layer, and the effect of 1 m crust layer were examined within this parametric study. In order to derive fragility curves, each variation of the model was loaded by at least eight intensities of a set of 30 ground motions. Permanent vertical displacement of middle point at embankment crest was selected as engineering demand parameter, while peak ground acceleration at bedrock and Arias Intensity were used as intensity measures. Threshold values for assessing three damage states, from minor to extensive deformations of the embankment, were taken from the literature (e.g. Oblak et al.[16]). Subsequently, this research will focus on the application of this proposal to the Barra Bridge approaching embankments. Even though the seismic hazard of the region is low, the presence of a sensitive structure, such as the bridge in question, justifies specific ground characterization and analysis of its performance in the event of soil liquefaction.

4. Conclusions

This paper addressed the site investigations and liquefaction analyses performed in Aveiro (Portugal), through CPT and DMT test.

The use of piezocone data in the CRR estimation is well known, while the dilatometer test has its relevancy due to the recognized sensitivity of K_D to a number of factors which are known to influence liquefaction resistance and are difficult to be detected by other tests.

There is a general good agreement between these methods for the estimate of the safety factor against liquefaction (FS_{liq}) and the liquefaction potential index (LPI). However, some disagreement was found, with respect to the liquefaction severity number (LSN) values. This depicts the need for further investigation on the most influencing factors, such as the fines content, not taken into account by current CRR-K_D correlations, as well as on the influence of lateral spreading.

The liquefaction assessment from CPTu and DMT test revealed a low liquefaction vulnerability for the Aveiro test site, when considering the seismic action 1, and a high liquefaction vulnerability if considering the second seismic action.

Acknowledgements

An appreciation to the Polytechnic Institute of Guarda for providing the equipment and material required for the site investigations and the Port of Aveiro for facilitating the access to the testing site.

The work presented in this article was supported by the Portuguese Foundation for Science and Technology (FCT), within the research project PTDC/ECM-Geo/1780/2014: "Liquefaction Assessment Protocols to Protect Critical Infrastructures Against Earthquake Damage (LIQ2PROEARTH)", financed by the European Commission Operational Competitiveness Program (COMPETE). The fourth author also acknowledges the support of FCT through SFRH/BD/146265/2019 grant. This work was also financially supported by: Base Funding - UIDB/04708/2020 of the CONSTRUCT – Instituto de I&D em Estruturas e Construções – funded by national funds through the FCT/MCTES (PIDDAC).

References

[1] Seed, H.B. & Idriss, I.M. 1971. Simplified procedure for evaluating soil liquefaction potential. J. Geotech. Engrg. Div., ASCE, 97(9):1249–1273.

[2] Iwasaki, T., Tatsuoka, F., Tokida, K. & Yasuda, S. 1978. A practical method for assessing soil liquefac- tion potential based on case studies at various sites in Japan. Proceedings of the 2nd International Conference on Microzonation. San Francisco, CA, USA, pp. 885–896.

[3] Iwasaki, T., Tokida, K., Tatsuoka, F., Watanabe, S., Ya- suda, S. and Sato, H. (1982). "Microzonation for soil liquefaction potential using simplified methods." Proc. of 3rd Int. Conf. on Microzonation, Seattle, 3, 1319–1330.

[4] Tonkin and Taylor, Ltd. (2013). "Liquefaction Vulnerability Study." Report to Earthquake Commission, Tand T ref. 52020.0200/v1.0, prepared by S. Van Ballegooy and P. Malan, available at https://canterburygeotechnicaldatabase.projectorbit.co m.

[5] Zhang, G., Robertson, P.K. & Brachman, R.W. 2002. Estimating liquefaction-induced ground settlements from CPT for level ground. Canadian Geotechnical Journal, 39(5), pp.1168–1180.

[6] NP EN 1998-1 (2010). "Eurocódigo 8 - Projecto de estruturas para resistência aos sismos. Parte 1: Regras gerais, acções sísmicas e regras para edifícios. " IPQ.

[7] NP EN 1998-5 (2010). "Eurocódigo 8 - Projecto de estruturas para resistência aos sismos. Parte 5: Fundações, estruturas de suporte e aspectos geotécnicos." IPQ.

[8] Idriss, I.M. 1999. An update to the Seed-Idriss simplified procedure for evaluating liquefaction potential. Proc. of the TRB Workshop on New Approaches to Liquefaction, Federal Highway Administration.

[9] Idriss, I. M., Boulanger, R. W. (2008). Soil liquefaction during earthquakes. Monograph MNO-12, Earthquake Engineering Research Institute, Oakland, CA, 261 pp.

[10] Boulanger, R.W. & Idriss, I.M. 2014. CPT and SPT based liquefaction triggering procedures. Report No. UCD/ CGM-14/01. Center for Geotechnical Modeling, University of California, Davis. 134 pp

[11] Marchetti, S. 2015. Incorporating the Stress History Parameter KD of DMT into the Liquefaction Correlations in Clean Uncemented Sands. Journal of Geotechnical and Geoenvironmental Engineering, Vol.142, Issue 2

[12] Idriss, I.M. and Boulanger, R.W. (2006). "Semi-empirical procedures for evaluating liquefaction potential during earthquakes" Soil Dyn. and Earthquake Eng., 26, 115-130

[13] Robertson, P.K. (2012). "Mitchell Lecture. Interpretation of in-situ tests - some insight." Proc. ISC-4, Porto de Galinhas - Brazil, 1, 3-24.

[14] Ferreira C, Viana da Fonseca A, Ramos C. Saldanha S. Amoroso S, Rodrigues C. Bull Earthquake Eng (2019). Online first https://doi.org/10.1007/s10518-019-00721-1

[15] van Ballegooy S, Malan P, Lacrosse V, Jacka ME, Cubrinovski M, Bray JD, O'Rourke TD, Crawford SA, Cowane H. Assessment of Liquefaction-Induced Land Damage for Residential Christchurch. Earthquake Spectra 2014; 30(1), 31-55.

[16] Oblak, A, Kuder, S, Logar, J, Viana da Fonseca, A (2019) Numerical assessment of fragility curves for embankments on liquefiable ground; XVII European Conference on Soil Mechanics and Geotechnical Engineering, Reykjavik, Iceland doi: 10.32075/17ECSMGE-2019-0899 (http://www.7icege.com/).